Thompson, R. E., Larson, D. R., and Webb, W. W. (2002). Precise nanometer localization analysis for individual fluorescent probes. *Biophys. J.* **82,** 2775–2783.

Tsien, R. Y. (2005). Building and breeding molecules to spy on cells and tumors. *FEBS Lett.* **579,** 927–932.

Ueda, M., Sako, Y., Tanaka, T., Devreotes, P., and Yanagida, T. (2001). Single-molecule analysis of chemotactic signaling in Dictyostelium cells. *Science* **294,** 864–867.

Yildiz, A., Forkey, J. N., McKinney, S. A., Ha, T., Goldman, Y. E., and Selvin, P. R. (2003). Myosin V walks hand-over-hand: Single fluorophore imaging with 1.5-nm localization. *Science* **300,** 2061–2065.

Weiss, S. (1999). Fluorescence spectroscopy of single biomolecules. *Science* **283,** 1676–1683.

Wu, X., Liu, H., Liu, J., Haley, K. N., Treadway, J. A., Larson, J. P., Ge, N., Peale, F., and Bruchez, M. P. (2003). Immunofluorescent labeling of cancer marker Her2 and other cellular targets with semiconductor quantum dots. *Nature Biotechnol.* **21,** 41–46.

[13] Development and Application of Automatic High-Resolution Light Microscopy for Cell-Based Screens

By YAEL PARAN, IRENA LAVELIN, SUHA NAFFAR-ABU-AMARA, SABINA WINOGRAD-KATZ, YUVALAL LIRON, BENJAMIN GEIGER, and ZVI KAM

Abstract

Large-scale microscopy-based screens offer compelling advantages for assessing the effects of genetic and pharmacological modulations on a wide variety of cellular features. However, development of such assays is often confronted by an apparent conflict between the need for high throughput, which usually provides limited information on a large number of samples, and a high-content approach, providing detailed information on each sample. This chapter describes a novel high-resolution screening (HRS) platform that is able to acquire large sets of data at a high rate and light microscope resolution using specific ''reporter cells,'' cultured in multiwell plates. To harvest extensive morphological and molecular information in these automated screens, we have constructed a general analysis pipeline that is capable of assigning scores to multiparameter-based comparisons between treated cells and controls. This chapter demonstrates the structure of this system and its application for several research projects, including screening of chemical compound libraries for their effect on cell adhesion, discovery of novel cytoskeletal genes, discovery of cell migration-related genes, and a siRNA screen for perturbation of cell adhesion.

METHODS IN ENZYMOLOGY, VOL. 414 0076-6879/06 $35.00
Copyright 2006, Elsevier Inc. All rights reserved.
DOI: 10.1016/S0076-6879(06)14013-6

Introduction

One of the primary challenges of biological research in the ''post-genomic era'' is a comprehensive understanding of the concerted action of multiple genes and their protein products in performing basic life processes. A fundamental requirement for studying such issues is the characterization of gene expression patterns, modification and subcellular localization of proteins and elucidation of their involvement in multiprotein complexes, and signaling networks within cells. It is noteworthy that in addition to their synthesis and spatial organization, protein assemblies are highly dynamic and undergo continuous rearrangement. Apparently many of these complex processes cannot be monitored effectively using purely biochemical approaches, which are well designed for assessing specific molecular interactions, yet they lack spatial resolution and are usually based on the collective behavior of cell populations. Such approaches fail to follow dynamic events in individual cells due to cell-to-cell heterogeneity and limited synchrony.

Many of the cellular features just mentioned can be monitored by advanced light microscopy, which has developed in recent years into an increasingly powerful tool for studying molecular and cellular events. Information about cells, which is attainable by microscopy, includes, for example, cell morphology, architectural organization of organelles, monitoring of gene expression (using promoter reporters), and localization of proteins (using fluorescently tagged fusion proteins). In addition, time-lapse recording, combined with fluorescence tracking, photobleaching, or photoactivation, can shed light on dynamic molecular processes in live cells.

A most compelling challenge is to harvest such quantitative structural and functional information from large numbers of samples. This need is a natural development of large genetic screens, where the effect of gene overexpression or suppression is tested using a wide variety of model systems, including yeast (Huh *et al.*, 2003), Drosophila (Boutros *et al.*, 2004), and human cells (Sachse *et al.*, 2005). Similar requirements are apparent in pharmacological screens, where libraries of chemical compounds are tested for their physiological effects (Clemons, 2004; Stockwell, 2004). In order to adapt the throughput to the number of screened samples, automation in microscopy is required, both in the acquisition and in the analysis stages. Moreover, each screen should provide specific information about a rather narrow slice of the multidimensional space characterizing the specific cellular systems. To resolve many features in a large number of samples, exhaustive screens are needed, which further emphasizes the need for suitable high-throughput and automated technology (Abraham *et al.*, 2004).

The implementation of advanced microscopy-based screening requires that the interpretation of data will be not only accurate, but also as fast as the rate of acquisition, and preferably online. Thus, quantitative analysis needs to deal with cell-to-cell variability based on an analysis of sufficiently large numbers of cells. This requirement further complicates the screening process, due to both the need to process highly elaborate images and the need to acquire and analyze a large number of images, sufficient for reliable statistical evaluation.

In view of these needs, many automatic microscope systems have been developed, some of which are available commercially (Smith and Eisenstein, 2005). Moreover, it is noteworthy that computerized analyses of microscope images have been amply described over the years, including the development of algorithms that can be applied to extract textural and morphological parameters from high-throughput experiments (Conrad *et al*., 2004; Mitchison, 2005; Murphy, 2005; Perlman *et al*., 2004, 2005; Tanaka *et al*., 2005; Yarrow *et al*., 2003; Zhou *et al*., 2005). However, the capacity to perform fast and automated data acquisition at high resolution, using high numerical aperture (NA) objectives (e.g., $\times 60$ NA $= 0.9$), combined with automated analysis pipeline, is still rather limited.

This chapter describes the design of a fully automated, high-throughput, high-resolution multiwell plate-scanning microscope platform and its application in several cell-based screening projects. We focus on cytoskeletal and cell adhesion sites, which play a central role in dynamic cellular events, including cell migration, tissue formation, and transmembrane signaling. Due to their importance, these cell structures are also attractive targets for a variety of drugs (Peterson and Mitchison, 2002). The system described here can acquire up to two images per second using objective magnifications up to $\times 100/0.9$ and focusing before each acquisition by a fast and robust laser-based AutoFocus device (Liron *et al*., 2006). An automated image analysis pipeline has been assembled with project-specific analysis routines and applied for identifying morphological and fluorescence intensity-related changes induced by genetic or chemical perturbations.

Technical Description

Microscope

The automated systems (Fig. 1) are based on IX71 and IX81 microscopes (Olympus, Japan). Microscope automation is provided by a ProScan system (Prior, Cambridge, UK) consisting of a stage, focus, objectives and dichroic cube changers, excitation and emission filter wheels, and shutters. Images are taken using a Quantix camera (Photometrics, Tucson, AZ),

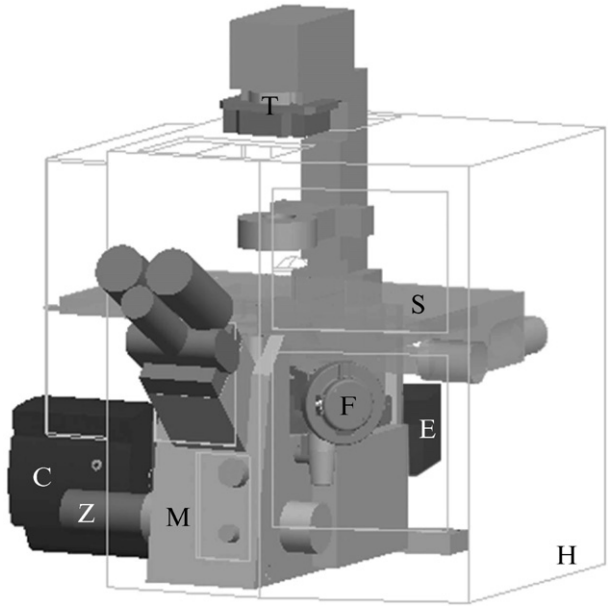

FIG. 1. A schematic representation of the high-resolution automated plate-screening microscope system. M, microscope body, Olympus IX81; S, XY stage and plate holder; Z, focus motor; C, camera with emission filter wheel; E, epi-illumination, including Hg arc lamp, shutter, and fluorescence excitation filter wheel; T, transmitted light halogen lamp and shutter; F, AutoFocus, optoelectronics; H, environmental chamber. Controlling electronics, computer, xyz joystick, monitor, and keyboard are not shown.

equipped with a Marconi (EEV) CCD57 back-illuminated chip with very high quantum efficiency in the visible and the near-IR (>80% quantum efficiency [QE] in 450- to 650-nm wavelength range). A manual focus jog and stage joystick are used for system alignment and initial setting of the screen.

For live cells screening, microscopes are equipped with a home-built Plexiglas box heated to 37° by an air circulator. CO_2 can be supplied, when necessary, via a small chamber encasing the multiwell plate. To allow gas exchange, without increased evaporation of the medium, the wells are covered by a Luminex BioFolie foil (Hanover, Germany).

The laser AutoFocus is a key component for the automated capabilities of the microscope. High-resolution imaging necessitates precise axial setting of the focus before each image is acquired, yet at minimal extra time and sufficient robustness to be repeated during long screens with negligible failure rates. These features were designed into our system (Liron *et al.*, 2006).

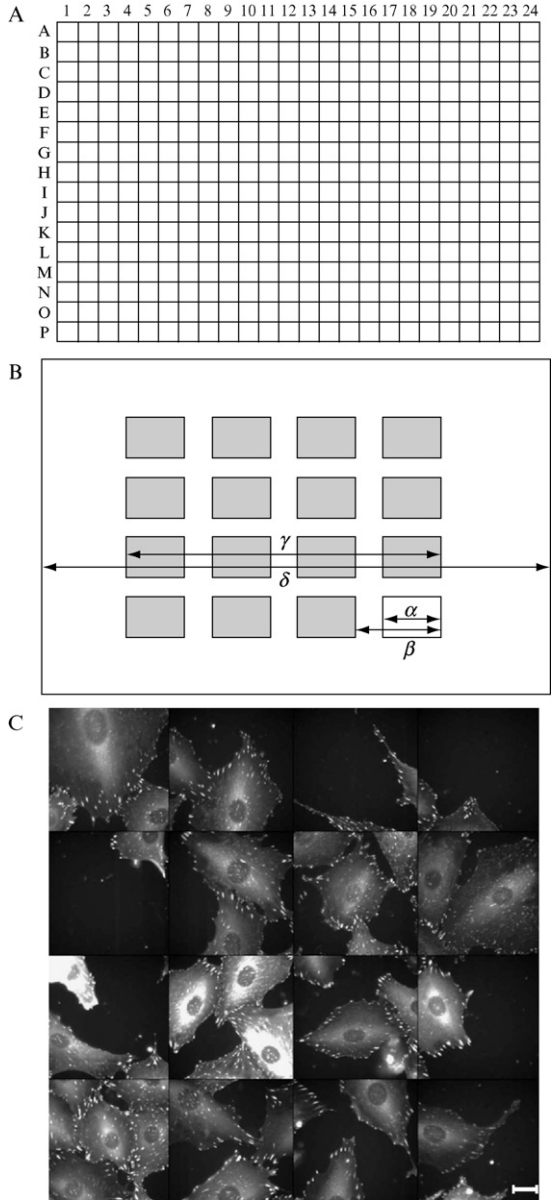

FIG. 2. (A) Plate graphic user interface (GUI). Graphics are used during automated acquisition to display the progress of the screen, for interactive visualization (mouse click on a well in a plate GUI displays montage of all images acquired in the well, and click on a field within a well displays the corresponding image in full resolution), and for display of analysis

Image Acquisition Software

The acquisition program, Resolve6D, organizes six-dimensional image files (i.e., X, Y, Z, wavelength, time, and position in the multiwell plate). It uses the UCSF Linux-based Image Visualization Environment and Priism software (IVE, http:/msg.ucsf.edu/IVE) for image display and Graphic User Interface. A command-line interpreter runs computer control sequences on all microscope functions, including objective changes, stage, focus, shutters, and filters, and allows unlimited depth of looping on all variables. Loops on wells are set by a selection of regions within all plate formats (96, 384, 1536 round or square wells). Within each well the imaged fields are defined by setting a fraction of the well area and a fill factor (>1 implies partially overlapping fields for matching image tiles into continuous carpets, see Fig. 2). The scanning program then chooses the acquisition path, minimizing distances between successive fields to reduce the time spent on AutoFocusing. One can also manually select a point list for revisiting interesting cells and record multiple time-lapse movies, as well as automatically depicting points of interest. For example, a list of coordinates for all the fluorescent cells can be extracted automatically from low-magnification images, which then may be revisited at high magnification. This multimagnification imaging capability can accelerate screens by factors of 10 or more when informative high-magnification images are scarce ($\sim$10%), such as in case of low-efficiency transfection.

Image Analysis

We developed an integrated solution for a data processing pipeline consisting of several analysis steps or modules. Image processing is highly image dependent. Development of open architecture is therefore a key issue in this stepwise design. The challenge is to build a generalized platform capable of incorporating a wide and adaptable range of image interpretation schemes and statistical analyses. We want to deal with low-, medium-, and high-magnification images of different cell types and with various assays based on morphology and subcellular distributions of tagged molecules and organelles. The modules are as follow.

Image Database Module

Microscope-based screens can produce Terabytes of high-resolution image data. We adopted the MRC file format (http://www.msg.ucsf.edu/IVE/

scores (coded in rainbow colors). (B) In-well imaged fields GUI. The fields distribution is determined by two parameters: filling factor $= \alpha/\beta$ and fraction of the well covered by images (γ/δ), as marked. (C) Montage of images acquired in one well. Scale bar: 20 μm.

IVE4_HTML/IM_ref2.html), which includes a header for global information about the experimental parameters, extended header for individual image information, and multiple images per file. This allows compact directory contents (file name annotates owner, date, and plate), with back-and-forth links between each condition or treatment (via plate/well numbers) and the corresponding images. The image files are associated with additional files created by the various analysis steps (e.g., montages, segmented object parameters, statistical scores, see later). Files are stored from the acquisition computers onto mass storage and accessed for analysis.

Interactive Visualization Module

Accessible visualization is a primary requirement for the researcher, for monitoring the acquisition, for inspecting controls, and for qualitatively evaluating effects. In addition, display of selected images, following automated computerized analysis, allows focusing on interesting samples. We base our visualization on whole well montages (tiling all images acquired in a well) called upon by plate and well numbers or via a plate–graphic interface (Fig. 2). A full-resolution display for each of the tiles can be called. Display windows have FIFO structure, keeping last displayed N images (N can be set), therefore allowing fast play of image sequences for the purpose of comparison.

Image Processing Module

Image processing is a mature field, nevertheless, biological image processing faces special needs that need to be addressed. The first requirement in microscopy is correction of the inhomogeneous illumination field. It can be achieved by a fiber optical scrambler spatially stabilizing the illumination intensity profile (Kam *et al*., 1993). However, the tight well walls perturb this profile, imposing development of alternative solutions. A second problem encountered in biological imaging is background, originating from optoelectronics, autofluorescence, nonlocalized diffuse labeling, and out-of-focus contributions. We use various processing schemes such as linear and nonlinear filtration, local contrast enhancement, and rolling-ball background estimates to "flatten" images prior to segmentation (Lichtenstein *et al*., 2003). It should be emphasized that the same image may be processed differently for segmentation of whole cell extents or for intracellular organelles. Simple and fast automated contrast-enhancement techniques are extremely useful also for visualization of the acquired images.

Image Segmentation and Connected Component Analysis Module

Segmentation and connected component analysis is the most common, but also most difficult approach to interpret image contents in terms of

"objects." Over the years we have developed and applied a number of segmentation algorithms based on adaptive thresholds: WaterShed (Zamir *et al*., 1999), fiber recognition (Lichtenstein *et al*., 2003), and multiscale algorithms (Sharon *et al*., 2001). The binary masks define objects, which are characterized by quantitative morphological and image intensity parameters (such as total and mean fluorescent intensity, area, axial ratio from best-fitted ellipsoid). Multicolor correlation analysis yields quantitative colocalization parameters (e.g., with a labeled organelle) (Kam *et al*., 2001). For cells expressing fluorescently tagged proteins, one can segment the overall cell body by the higher diffuse fluorescence compared to the cell-free surrounding. Specific tags, labeling intracellular structures, can be used to evaluate proliferation, survival, and death and to recognize, at low resolution, cell locations for further analyses. Detailed quantification parameters for intracellular features, such as the nucleus and its substructures, cytoskeletal fibers, endoplasmic reticulum, Golgi, and mitochondria, serve as excellent reporters for cell phenotyping and identification of anomalous morphologies.

Statistical Module

A major feature of cell-based screens is the large cell-by-cell variability. We rely on statistics to find an optimal balance between the desired high throughput and the required high sensitivity and resolution. We feed the outputs of the quantitative parameters for all segmented individual objects into analyses, which are capable of accumulating data from multiple images (one or many wells) and rejecting outliers. The module exports cumulative characterization as histograms, scatter plots, percentiles, and so on for each parameter and for all the analyzed wells.

Multiparametric Scoring of Changes in Treated versus Control Cells

This module compares each "test well" to controls and supplies scores, nominating the wells that were affected by the treatment. Such scores are commonly defined in nonparametric statistical methods by comparing two lists of variables (e.g., Komologov–Smirnov and rank sum tests). For our screen analysis purpose, we extended these tests for histograms. In addition, we utilized comparison of median and other percentiles, which were found useful to characterize far from normal distributions and cases where few extreme events are to be weighted heavily or median behavior shifts are expected. We also compared two parameter domains (quadrants), similar to definition of subpopulations in flow cytometry scatter plots (Boddy *et al*., 2001). We have good grounds to propose that multiparameter scores will depict variable changes that a single parameter test may overlook. We therefore apply different multiparametric schemes for

scoring differences between an experimental well and controls, including ranking and clustering of multiparameter vectors (Zamir *et al*., 2005). The purpose of this process is to grade all wells according to the degree of changes and to characterize the parameters mostly aberrant compared to the controls. This analysis links directly to the original images, supplying convenient visualization to survey the results (detailed description of the analysis is described elsewhere).

Biological Screens

Screening projects are aimed at quite diverse goals. They can address a wide variety of cellular processes and/or structures and use a wide range of genetic or chemical perturbations. This section describes several automatic, cell-based screens for a variety of research projects, including screens for adhesion- and cytoskeleton-perturbing chemical compounds, a search for novel structural cellular proteins, and analysis of cell migration.

Perturbation of Cell Adhesions

A common application of automated microscopic systems is cell-based screening of cell-perturbing agents. This section describes two kinds of perturbation screens, both targeting focal adhesions in cultured cells: a chemical compounds screen and a siRNA screen. Both screens used reporter cell lines expressing fluorescently tagged paxillin, a prominent component in the focal adhesion (FA) complex. It is noteworthy that FAs are involved in the anchoring of cells to the substrate, as well as in the transduction of adhesion-induced signals and regulation of actin organization within cells.

Chemical Compounds Screens

A search for novel drugs that might interfere with cellular functions has been approached in recent years by screening diverse chemical libraries and their modifications. Examination of the drug effect on live cells, including effects on cellular morphology and relocation of structural and signaling proteins, requires microscope-based imaging at high resolution. The higher the image resolution, the more sensitive the readout of drug effects on cellular functions manifested as subtle cell architectural attributes. Here we examine the effects of the chemical compound library on FAs. REF52 cells expressing stably paxillin-yellow fluorescent protein (YFP) served as reporter cells. Cells are cultured in multiwell plates and treated by compounds from a library of 10,000 low molecular weight, chemically defined molecules (ChemDiv Inc., San Diego, CA) using a single compound per well. Following treatment, cells are fixed and plates are screened for effects on FAs on the automated microscope

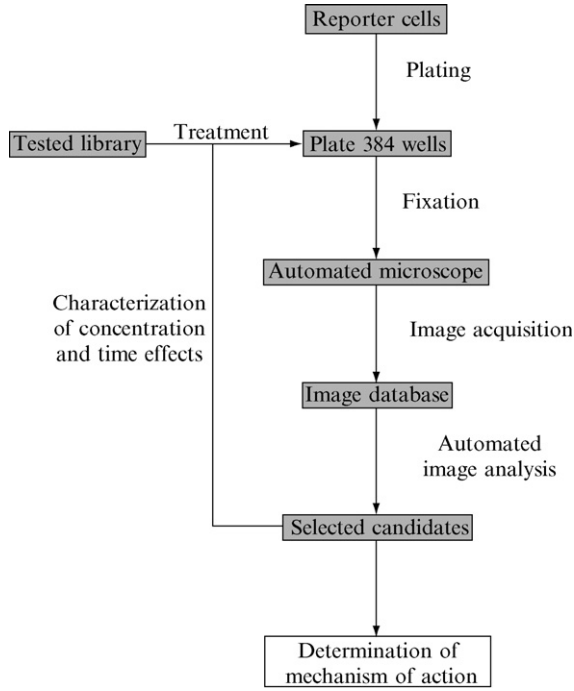

FIG. 3. Flowchart of the perturbation screen process.

at high resolution (Fig. 3). Acquired images are subjected to quantitative analysis, which yields more than 100 compounds with interesting cytoskeletal and FA-perturbing effects (see database of the screen results at http://www.weizmann.ac.il/mcb/Geiger/Screening.html). Major perturbations include FA elongation, reduction in FA size, loss of FAs at the cell center, abnormal paxillin localization, and overall cytoskeletal collapse (Fig. 4). The automated microscope is also utilized to study, in detail, the time- and concentration-dependent effects of selected compounds and their mechanism of action using labeling of cytoskeletal and FA-related proteins (Fig. 3).

Protocol for Cell-Based FA Perturbation Screening

1. REF52 cells, stably expressing paxillin-YFP, are seeded [800 cells/well in 50 μl Dulbecco's Modified Eagle's Medium (DMEM) with 10% fetal calf serum (FCS) and antibiotics] and cultured in optical bottom, 384-well plates (Greiner bio-one GmbH, Fricjkenhausen, Germany. F-bottom, μClear, black, tissue-culture treated).

2. Following a 24-h incubation, cells are treated with chemical compounds at a concentration of 10 μM (diluted from stock solution with DMEM containing 10% FCS and antibiotics).

3. Following a 90-min incubation, cells are fixed by dipping the plate in 3% paraformaldehyde bath for 25 min and then washing three times with phosphate-buffered saline (PBS).

4. Plates are examined by an automated microscope (objective $\times$ 60/0.9, 1-s exposure). In each well 16 images are acquired.

5. The image database is subjected to processing, segmentation, and analysis, which highlight the selected hits for significant FA perturbations.

siRNA Screen

To explore the mechanism involved in focal adhesion formation, individual signaling and focal adhesion complexes were knocked down using siRNA technology (Schutze, 2004). For that purpose, HeLa JW cells, expressing paxillin-YFP, were transfected with a library of "SMARTpools" RNA duplexes, each consisting of a mixture of four siRNAs, targeting the same gene (Dharmacon, USA). The details concerning this screen are

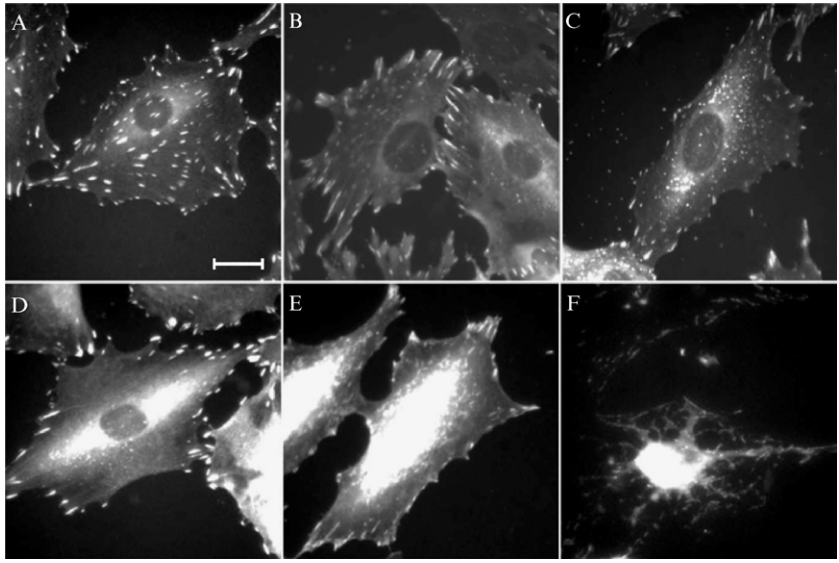

FIG. 4. Examples of focal adhesion perturbation patterns observed using the chemical compounds screen. (A) Untreated REF52 cells expressing paxillin-YFP. (B) Focal adhesion (FA) elongation. (C) Increase in number and decrease in size of FA. (D) Loss of FA at the cell center (usually associated with larger peripheral FA). (E) Increase in FA signal intensity and high amount of unlocalized paxillin-YFP. (F) Major cell damage. Scale bar: 20 μm.

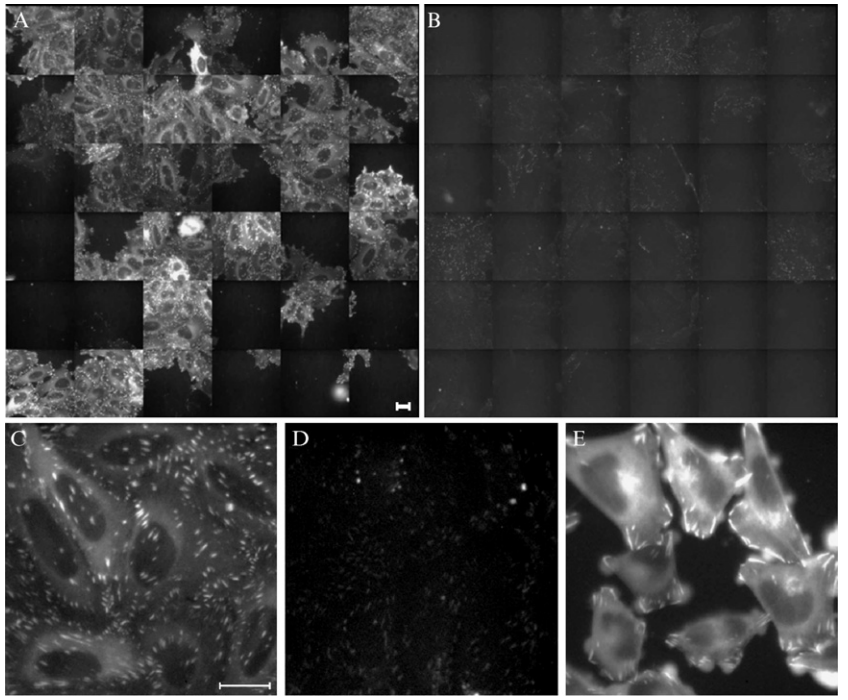

FIG. 5. Examples of images from siRNA screen. (A) Montage of images of untransfected reporter cells (HeLa cells expressing YFP-paxillin). (B) Montage of images of reporter cells transfected with siRNA targeting paxillin. (C) Single image of untransfected reporter cells. (D) Single image of cells transfected with siRNA targeting paxillin. (E) Single image of cells transfected with siRNA targeting talin. Scale bar: 20 μm.

beyond the scope of this chapter; however, the use of automatic microscopy was mandatory for screening the effects of a large number of siRNA duplexes. Thus, following treatment with the specific siRNA, cells were fixed and their FAs recorded using the automated microscope (Fig. 3). Major cytoskeletal changes detected in this screen include reduction in FA number and/or size, changes in FA localization within the cells, and overall effect on cell spreading and polarization. Figure 5 shows images of non-transfected cells, cells transfected with siRNA targeting paxillin, and cells transfected with siRNA targeting talin. Transfection with paxillin leads to a decrease in focal adhesion intensity as expected from the decrease in the expression of the YFP-tagged paxillin. The image of cells treated with talin siRNA is an example of the dramatic change in FA distribution and morphology following the treatment (detailed description of this screen will be published elsewhere).

Protocol for the Screening of siRNA Library

1. HeLa JW cells, stably expressing paxillin-YFP, are seeded in fibronectin-coated 384-well microplates (250 cells/well in 50 μl DMEM 10% FCS without antibiotics).

2. Following a 24-h incubation, cells are transfected with 100 n*M* siRNA using oligofectamine (Invitrogen, USA). SiRNA is diluted in DMEM without serum to 10 μl final volume.

3. Oligofectamine is diluted 1:10 in medium. After 5 min 10 μl of the Oligofectamine–DMEM mixture is mixed with each siRNA and the mixture is incubated for 20 min.

4. Medium (30 μl) is removed from each well with HeLa cells, and 5 μl of the siRNA Oligofectamine mix is added to the cells.

5. Cells are fixed 72 h after transfection with 3% paraformaldehyde and examined by the automatic microscope system.

6. Each plate contains, in addition, wells with cells transfected with siControl pool (a nontargeting siRNA), cyclophylin siRNA, and siTOX for transfection efficiency control. Transfection efficiency (calibrated to 80 to 90% in our case) is assessed by cell survival after siTOX transfection.

7. Plates are examined by the automated microscope (objective $\times$ 60/0.9, 1.5-s exposure). In each well 36 images are acquired and analyzed to extract FA affective genes.

A cDNA screen for Identifying Novel Structural Cellular Proteins Based on Localization of YFP-Fusion Proteins

One of the applications of the automated microscope system is a visual screen that aims at the identification of novel proteins, according to their subcellular localization. For that purpose, a normalized, oriented cDNA library was constructed with poly(A)-primed cDNA, prepared from mixed mRNA of rat brain tissue and rat kidney fibroblast (RKF) cell line, randomly fragmented to an average insert size of 500 bp. These fragments were cloned into pLPCX retroviral vector (Clontech) using *Sfi*I sites upstream to the YFP cDNA. The cDNA libraries contain 0.5–2 $\times$ 10^6 clones, more than 50% of which have cDNA insertions.

To screen the expression library we infected REF52 cells with pools of clones generated by subdividing the library. Those clones that contained upstream open reading frames out of frame with YFP were excluded from the subsequent analysis by FACS sorting. Cells expressing YFP fusion proteins were plated 5 cells per well in 96-well plates. Each well is then ''backed up'' and frozen in a 96-well plate for future investigation, as well as plated into 384 plates with optical plastic bottoms for screening for

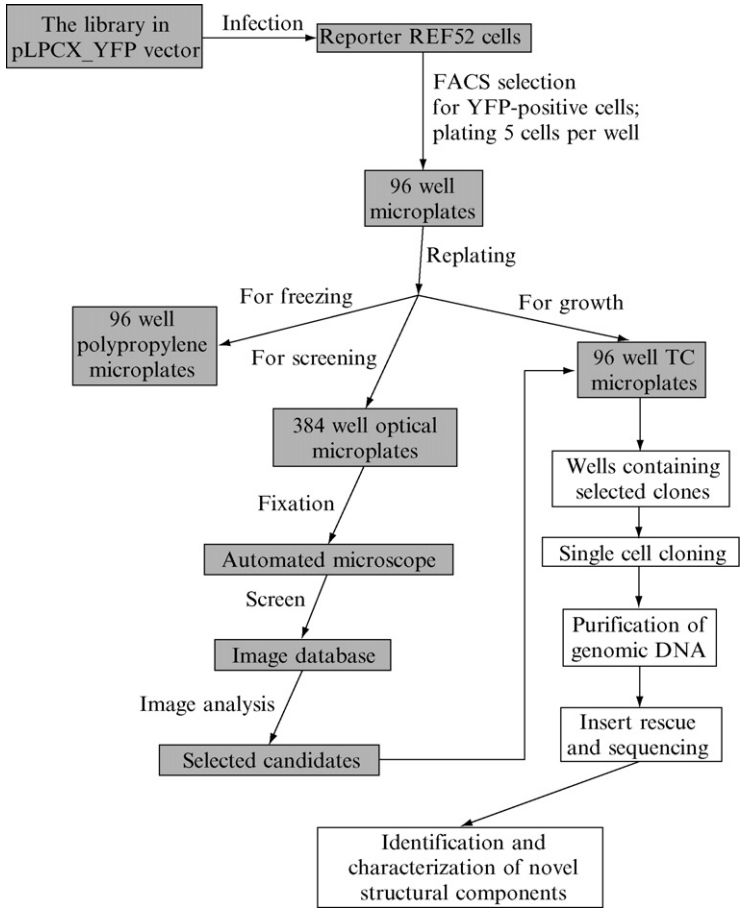

FIG. 6. Flowchart of the protein localization screen.

distinct patterns of YFP fluorescence by the automated microscope. Cells from wells displaying patterns of interest were then subjected to single-cell cloning and rescreened to isolate the clone responsible for the distinct pattern. Genes of interest were cloned, sequenced, and subjected to further characterization (Fig. 6). About 4% of total infected cells had visible cellular localization of the exogenous proteins representing cell structures such as nucleus, Golgi complex, mitochondria, and others. As expected, a significant percentage of the cDNA products localized to the cytosol (20% of the proteins showed definite localization) and the nucleus (15%), and

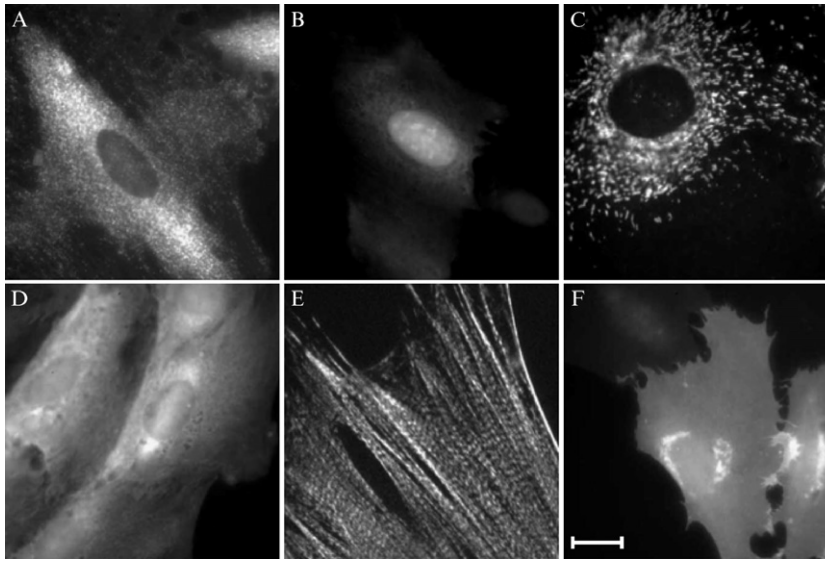

FIG. 7. Examples of subcellular localizations of YFP-fusion proteins observed in localization screening. (A) Vesicules, (B) nuclear, (C) mitochondrial, (D) cytoplasmic, (E) stress fibers, and (F) membrane. Scale bar: 20 μm.

about 20% were found to be associated with the secretory pathway (see database of the screen results at http://www.weizmann.ac.il/mcb/Geiger/Screening.html). Figure 7 shows a few examples of the subcellular localizations observed in the experiments.

Protocol for cDNA Screening

1. cDNA library (10 mg) in the pLPCX_YFP vector are used for infection of 3×10^6 target REF52 cells. Infection efficiency is titrated to about 80% to prevent insertion of multiple inserts.

2. Three days after infection, cells expressing YFP are selected by FACS and plated in a 96-well plate (5 cells/well) and mixed with naive cells (500 cell/well) for cells with growth problems at low confluence. Cells are then cultured to 100% confluence.

3. Puromycin (2 μg/ml) is added to select colonies of the infected cells (5 colonies per well). Cells are cultured to 80 to 100% confluence.

4. Cells from each well are replated to three plates: (1) 384-well plate with optical bottom for screening; (2) 96-well polypropylene plate for immediate freezing in liquid nitrogen (''back-up''); and (3) 96-well regular cell culture plate for following cell growth (''growing plate'').

5. The next day cells in the 384-well plate are fixed by dumping the plate in a 3% paraformaldehyde bath for 25 min and are then washed three times with PBS.

6. The plate is transferred to the automated microscope (objective × 60/0.9, exposure 1.5 s, 25 to 36 fields per well).

7. Montages are prepared for visual selection of clones displaying YFP-labeled subcellular patterns of interest (positive clones).

8. Cells from wells in the 96-well ''growing plate,'' corresponding to 384-plate wells containing positive clones, are transferred to new dishes for single-cell cloning and rescreening for isolation of clones responsible for the distinct patterns.

9. Genomic DNA from each single positive clone is purified and the cDNA inserts are rescued by polymerase chain reaction for sequencing, identification, and future characterization.

Screening for Genes Affecting Cell Migration

Cell migration is essential for the development and maintenance of normal tissues and organs; furthermore, enhanced migratory activity is common in malignant cells and is believed to be involved in metastasis. In order to identify proteins involved in or affecting cancer-related cell migration, we developed a quantitative high-throughput method for assessing cell motility. Many methods have been employed to measure two- and three-dimensional cell migration (Boyden, 1962; Hallab *et al*., 2000; Lee *et al*., 2000; Tamura *et al*., 1998; Zigmond, 1977). However, high-throughput screening for cell motility demands the use of assays that record time-dependent changes in cell position, such as time-lapse movies, wound healing, or phagokinetic track formation (Albrecht-Buehler, 1977). The latter was our method of choice, using polystyrene beads, rather than the original colloid gold particles. Glass-bottom 96-well plates were coated with a monolayer of microbeads and then cells expressing different genes were seeded on the bead monolayer and incubated for several (5 to 9) hours and then fixed and examined. Transmitted light images (×10 objective) of adjacent fields recording the entire surface of the well were acquired and ''stitched'' together to form a continuous montage. This enabled us to view all the tracks throughout the entire well. The images exhibit smooth gray background, with bead-cleared tracks observed as brighter regions. Cells were recognized by the phagocytosed beads usually concentrated around the nucleus. Different cell lines produce characteristically different track shapes, for example, elongated or round, with smooth or rough border, reflecting their migratory behavior (Fig. 8). Computerized analysis of the

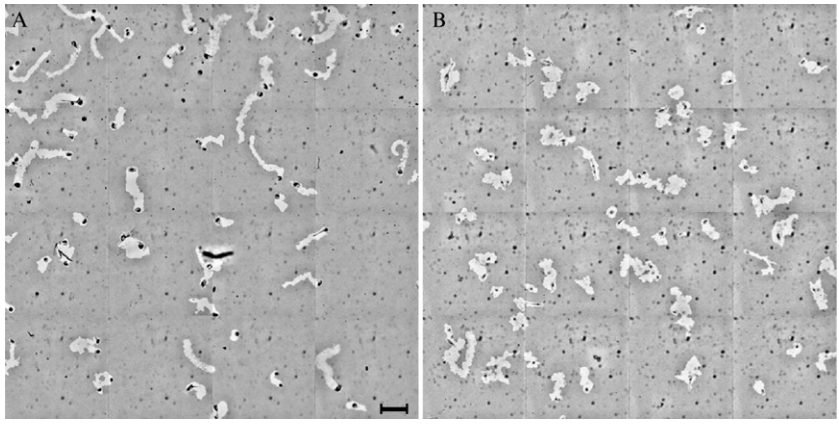

FIG. 8. Phagokinetic tracks of H1299 (nonsmall cell lung carcinoma) and MDA-MB-231 (metastatic breast cancer) cell lines. (A) H1299 cells present thin and elongated tracks, indicating persistent migration, compared to (B) the wide and short tracks of e MDA-MB-231 cells. Scale bar: 200 μm.

track morphology using multiscale segmentation methods allowed extraction of gross track parameters (area, maximum length, ratio between long and short axes of best-fitted ellipsoid), as well as detailed perimeter and border roughness features (detailed description of the screen for migration-inducing genes and track analysis will be published elsewhere).

Protocol for Motility Assay

1. Glass-bottom 96-well plates (Whatmann) are covered with 50 μl fibronectin (Sigma Chem. Co. F-1141; 10 μg/ml in PBS) and incubated overnight at 40°, washed twice with 200 μl PBS using a plate washer (Colombus plus, Tecan, Switzerland), and left with 50 μl PBS in each well.

2. White polystyrene latex 0.34-μm-diameter beads (product number 2–300, batch number 1344, Interfacial Dynamics Corporation/Molecular Probes Microspheres Technologies, Oregon) are sedimented by centrifugation (2 $\times$ 5 min at 14,000 rpm) and resuspended in PBS to a final concentration of 0.9×10^{12} beads/ml. The PBS that kept the wells wet is replaced by 70 μl of beads solution, and the plate is incubated at 37° for 2 h. The wells are then washed gently with PBS using the plate washer. After the last wash, 70 μl of PBS is left in each well.

3. PBS is replaced with 50 μl of culture medium. One hundred fifty to 250 cells suspended in a volume of 50 μl are spread gently and evenly over each well area using a multichannel micropipette and incubated to perform their motility at 37°, 5% CO_2 for 5 to 9 h (depending on the cell type).

4. Following incubation, the cells are fixed in 3% paraformaldehyde for 15 min and washed twice with PBS.

5. Fixed plates are imaged by the automated microscope, and the images are analyzed for tracks characterization.

Prospectives

This chapter outlined the development of screening systems and procedures enabling high-throughput analysis of cellular samples (i.e., in the order of thousands of samples per hour), associated with harvesting of high-resolution or ''high-content'' information. The development of such systems and their wide application requires a dedicated multidisciplinary effort, combining essential biological input, needed for the development of suitable ''reporter cells,'' with innovative know-how of microscope optics and mechanics and advanced image processing. Systems based on such combined expertise are likely to have considerable impact on basic biological research as well as on a variety of biomedical applications. High-resolution automated microscopy can provide valuable information on cutting-edge topics such as functional genomics, enabling the characterization of the cellular action of multiple genes, systems biology, probing the concerted action of multiple biological networks, and more. Novel biomedical applications are also likely to benefit greatly from advanced automated microscopy. This includes drug discovery and development processes, based on primary or secondary microscopy-assisted screens of chemical libraries, or comprehensive analysis of genetic factors affecting drug responsiveness. Naturally, to fully develop the approach described here for large genomic or pharmacological screens, one needs to further develop the automation of the screen, by setting robotic procedures for plate preparation, and processing, and improve the throughput of the microscope. It is also essential to install a fast on-line image acquisition and analysis system capable of quantification of fine changes in multiple cellular features. Given the wide recent interest in such systems it is anticipated that automated microscopy will be developed into one of the important tools in biomedical research.

Acknowledgments

The development of the screening systems was supported by NIGMS, National Institutes of Health Cell Migration Consortium Grant U54 GM64346 and the Israel Science Foundation (to BG) and the Binational Science Foundations (to ZK). Development of the automated system was supported by the Kahn Fund for Systems Biology at the Weizmann Institute of Science. BG holds the E. Neter Chair in Cell and Tumor Biology, and ZK is the Israel Pollak Professor in Biophysics.

References

Abraham, V., Taylor, D., and Haskins, J. (2004). High content screening applied to large scale cell biology. *Trends Biotech.* **22,** 15–22.

Albrecht-Buehler, G. (1977). The phagokinetic tracks of 3T3 cells. *Cell* **11,** 395–404.

Boddy, L., Wilkins, M. F., and Morris, C. W. (2001). Pattern recognition in flow cytometry. *Cytometry* **44,** 195–209.

Boutros, M., Kiger, A. A., Armknecht, S., Kerr, K., Hild, M., Koch, B., Haas, S. A., Consortium, H. F., Paro, R., and Perrimon, N. (2004). Genome-wide RNAi analysis of growth and viability in Drosophila cells. *Science* **303,** 832–835.

Boyden, S. (1962). The chemotactic effect of mixtures of antibody and antigen on polymorphonuclear leucocytes. *J. Exp. Med.* **115,** 453–466.

Clemons, P. A. (2004). Complex phenotypic assays in high-throughput screening. *Curr. Opin. Chem. Biol.* **8,** 334–338.

Conrad, C., Erfle, H., Warnat, P., Daigle, N., Lorch, T., Ellenberg, J., Pepperkok, R., and Eils, R. (2004). Automatic identification of subcellular phenotypes on human cell arrays. *Genome Res.* **14,** 1130–1136.

Hallab, N., Jacobs, J. J., and Black, J. (2000). Hypersensitivity to metallic biomaterials: A review of leukocyte migration inhibition assays. *Biomaterials* **21,** 1301–1314.

Huh, W. K., Falvo, J. V., Gerke, L. C., Carroll, A. S., Howson, R. W., Weissman, J. S., and O'Shea, E. K. (2003). Global analysis of protein localization in budding yeast. *Nature* **425,** 686–691.

Kam, Z., Jones, M. O., Chen, H., Agard, D., and Sedat, J. (1993). Design and construction of an optimal illumination system for quantitative wide field multidimensional microscopy. *Bioimaging* **1,** 71–81.

Kam, Z., Zamir, E., and Geiger, B. (2001). Probing molecular processes in live cells by quantitative multidimensional microscopy. *Trends Cell Biol.* **11,** 329–334.

Lee, H., Goetzl, E. J., and An, S. (2000). Lysophosphatidic acid and sphingosine 1- phosphate stimulate endothelial cell wound healing. *Am. J. Physiol. Cell Physiol.* **278,** C612–C618.

Lichtenstein, N., Geiger, B., and Kam, Z. (2003). Quantitative analysis of cytoskeletal organization by digital fluorescent microscopy. *Cytometry A* **54,** 8–18.

Liron, Y., Paran, Y., Geiger, B., and Kam, Z. (2006). Laser autofocusing system for high-resolution cell biological imaging. *J. Microscopy* **221,** 145–151.

Mitchison, T. J. (2005). Small-molecule screening and profiling by using automated microscopy. *Chembiochem.* **6,** 33–39.

Murphy, R. F. (2005). Cytomics and location proteomics: Automated interpretation of subcellular patterns in fluorescence microscope images. *Cytometry A* **67A,** 1–3.

Perlman, Z. E., Mitchison, T. J., and Mayer, T. U. (2005). High-content screening and profiling of drug activity in an automated centrosome-duplication assay. *Chembiochem.* **6,** 145–151.

Perlman, Z. E., Slack, M. D., Feng, Y., Mitchison, T. J., Wu, L. F., and Altschuler, S. J. (2004). Multidimensional drug profiling by automated microscopy. *Science* **306,** 1194–1198.

Peterson, J. R., and Mitchison, T. J. (2002). Small molecules, big impact: A history of chemical inhibitors and the cytoskeleton. *Chem. Biol.* **9,** 1275–1285.

Sachse, C., Krausz, E., Kronke, A., Hannus, M., Walsh, A., Grabner, A., Ovcharenko, D., Dorris, D., Trudel, C., Sonnichsen, B., and Echeverri, C. J. (2005). High throughput RNA interference strategies for target discovery and validation by using synthetic short interfering RNAs: Functional genomics investigations of biological pathways. *Methods Enzymol.* **392,** 242–277.

Schutze, N. (2004). siRNA technology. *Mol. Cell. Endocrinol.* **213,** 115–119.

Sharon, E., Brandt, A., and Basri, R. (2001). Segmentation and boundary detection using multiscale intensity measurements. *In* "IEEE Comput. Soc. Conf. Comput. Vision Pattern Recognit.," pp. 1469–1476.

Smith, C., and Eisenstein, M. (2005). Automated imaging: Data as far as the eye can see. *Nature Methods* **2,** 547–555.

Stockwell, B. R. (2004). Exploring biology with small organic molecules. *Nature* **432,** 846–854.

Tamura, M., Gu, J., Matsumoto, K., Aota, S., Parsons, R., and Yamada, K. M. (1998). Inhibition of cell migration, spreading, and focal adhesions by tumor suppressor PTEN. *Science* **280,** 1614–1617.

Tanaka, M., Bateman, R., Rauh, D., Vaisberg, E., Ramachandani, S., Zhang, C., Hansen, K. C., Burlingame, A. L., Trautman, J. K., Shokat, K. M., and Adams, C. L. (2005). An unbiased cell morphology-based screen for new, biologically active small molecules. *PLoS Biol.* **3,** e128.

Yarrow, J. C., Feng, Y., Perlman, Z. E., Kirchhausen, T., and Mitchison, T. J. (2003). Phenotypic screening of small molecule libraries by high throughput cell imaging. *Comb. Chem. High Throughput Screen* **6,** 279–286.

Zamir, E., Geiger, B., Cohen, N., Kam, Z., and Katz, B. Z. (2005). Resolving and classifying haematopoietic bone-marrow cell populations by multi-dimensional analysis of flow-cytometry data. *Br. J. Haematol.* **129,** 420–431.

Zamir, E., Katz, B. Z., Aota, S., Yamada, K. M., Geiger, B., and Kam, Z. (1999). Molecular diversity of cell-matrix adhesions. *J. Cell Sci.* **112**(Pt 11), 1655–1669.

Zhou, X., Cao, X., Perlman, Z., and Wong, S. T. (2006). A computerized cellular imaging system for high content analysis in Monastrol suppressor screens. *J. Biomed. Inform.* **39**(2), 115–125.

Zigmond, S. H. (1977). Ability of polymorphonuclear leukocytes to orient in gradients of chemotactic factors. *J. Cell Biol.* **75,** 606–616.

[14] Adenoviral Sensors for High-Content Cellular Analysis

By JONATHAN M. KENDALL, RAY ISMAIL, and NICK THOMAS

Abstract

To maximize the potential of high-content cellular analysis for investigating complex cellular signaling pathways and processes, we have generated a library of adenoviral encoded cellular sensors based on protein translocation and reporter gene activation that enable a diverse set of assays to be applied to lead compound profiling in drug discovery and development. Adenoviral vector transduction is an efficient and technically simple system for expression of cellular sensors in diverse cell types, including primary cells. Adenoviral vector-mediated transient expression of cellular sensors, either as fluorescent protein fusions or live cell gene reporters, allows rapid assay development for profiling the activities of

METHODS IN ENZYMOLOGY, VOL. 414 0076-6879/06 $35.00
Copyright 2006, Elsevier Inc. All rights reserved.
DOI: 10.1016/S0076-6879(06)14014-8